DEFORMATION OF AUGUSTINE VOLCANO, ALASKA, 1992-2006, MEASURED BY ERS AND ENVISAT SAR INTERFEROMETRY

Chang-Wook Lee* [1][2], Zhong Lu[1] and Oh-Ig Kwoun[1]

[1]SAIC, U.S. Geological Survey (USGS) Center for Earth Resources Observation and Science (EROS), Sioux Falls, South Dakota, 57198, USA, e-mail: crystalseven@yonsei.ac.kr
[2]Department of Earth System Sciences, Yonsei University, 134 Shinchon-dong, Seodaemun-gu, Seoul, 120-749, Korea

ABSTRACT ... Augustine volcano is an active stratovolcano located southwest of Anchorage, Alaska. Augustine volcano experienced seven significantly explosive eruptions in 1812, 1883, 1908, 1935, 1963, 1976, and 1986, and a minor eruption in January 2006. To measure ground surface deformation of Augustine volcano, we applied satellite radar interferometry with ERS-1/2 and ENVISAT SAR images acquired from three descending and three ascending satellite tracks. Multiple interferograms are stacked to reduce artifacts due to changes in atmospheric condition and retrieve temporal deformation sequence. For this, we used Least Square (LS) method for reducing atmospheric effects and Singular Value Decomposition (SVD) method for the retrieval of a temporal deformation sequence. Interferograms before 2006 eruption show about 3 cm/year subsidence by contraction of pyroclastic flow deposits from the 1986 eruption. Interferograms during 2006 eruption do not show significant deformation around volcano crater. Interferograms after 2006 eruption show again a several cm subsidence by compaction and contraction of pyroclastic flow deposits for a few months. This study demonstrates that satellite radar interferometry can monitor deformation of Augustine volcano to help understand the magma plumbing system driving surface deformation.

KEY WORDS: Interferometry, Atmospheric effects, Pyroclastic flow deposits, Subsidence

1. INTRODUCTION

Augustine Volcano is a 1250 m-high (Christopher et al., 1998) and 92km^2-size (Masterlark et al., 2006) stratovolcano in southwestern Cook Inlet about 290 kilometers southwest of Anchorage, Alaska (Figure 1). The Volcano is most frequently active and the youngest in the Cook Inlet volcanoes of Alaska (Beget et al., 2006) which was formed Jurassic and Cretaceous sedimentary strata and overlain by granitoid glacial erratics and volcanic hyaloclastites (Miller et al., 1998).

Augustine Volcano has experienced seven significantly explosive eruptions in 1812, 1883, 1935, 1963, 1976 and 1986, and a minor eruption in January 2006. The most violent eruption of Augustine Volcano was the 1883 eruption and it might be generated a tsunami with 7.5 – 9 m wave heights (Miller et al., 1998). Augustine Volcano has several kinds of volcanic hazards. Volcanic ash clouds of Augustine Volcano tend to erupt explosively, these ash clouds are a hazard to all aircraft downwind from the volcano (Casadevall, 1994). Volcanic ash fallout and volcanic bombs may be hazard to public health for south-central Alaska resident and low-flying aircraft (Christopher et al., 1998). Augustine Volcano is potentially capable of initiating tsunamis by earthquakes, pyroclastic flows entering the water, and volcanic debris avalanches and so on (Christopher et al., 1998). After 2-decades of 1986 eruption, the volcano had 13 explosive eruptions during 20-days from 11 January 2006 (Power et al., 2006). It was precursory period (pre-eruption stage) from May 2005 to 11 January 2006, the explosive period (co-eruption stage) from 11 to 28 January and the effusive period (post-eruption stage) from 2 February to late March (Power et al., 2006).

Spaceborne Synthetic Aperture Radar (SAR) repeat-pass interferometry has proven to be an effective tool for detecting surface deformation caused by volcanic activities, earthquakes, landslide and ground subsidence (Massonnet et al., 2000; Fruneau et al., 1996). It can be detected sub-centimeter changes on the ground surface with a very wide range of applications (Tarayre et al., 1996).

Here, we use the differential interferometry (DInSAR) method to monitor surface deformation occurring around the Augustine Volcano, Alaska. It can observe the surface displacements for the reservoir pressure decreases during the eruption and increases after the eruption by magma movement.

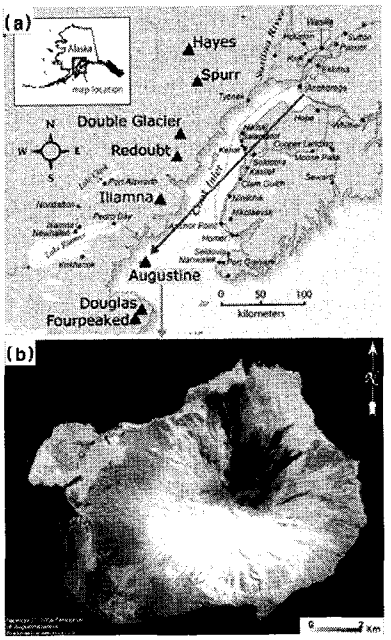

Figure. 1. Study area (Augustine Island) is located in the southwestern portion of the Cook Inlet, Alaska. (a) shows Augustine Island. (b) displays an aero-map over Augustine island by an airplane.

2. DATA AND ANALYSIS

2.1 Radar images and DEM

We made interferograms spanning the period from 1992 to present using ERS-1/2 repeat-pass data from 6 tracks and from 2003 to present using ENVISAT repeat-pass data. We used the 30m Shuttle Radar Topography Mission (SRTM) DEM to create differential interferogram.

2.2 InSAR results (before 2006 eruption)

SAR interferograms was acquired around 4 months (from June to October), because the Augustine volcano is covered by snow and ice during 6 or 7 months of the year. As a result of applying two-pass InSAR method using ERS-1 and ERS-2 SAR data, we constructed 15 interferograms that cover approximately one year span the period from 1992 to 2005 with good quality (Figure. 2). On the northern area of Augustine Island, 1 or 2 fringes are visible in the every interferogram. This deformation is probably due to the gravitational porosity compaction of pyroclastic flow deposits from 1986's eruption and thermoelastic contraction of the deposits over time. As with ERS-1 and ERS-2 interferograms, we constructed ENVISAT interferograms. The ENVISAT interferograms covering the period from 2003 to 2005 have the good quality (Figure 3). They have a term of around 1-year and as with the ERS interferograms we can count 1 or 2 fringes in the northern portion of Augustine Island.

2.3 Least square & Singular value decomposition method

Atmospheric artifacts, baseline decorrelation and unwrapping errors in the interferograms will be converted into errors in the calculated deformation at each pixel. Among of these errors, greatest source of error on the interferograms is often plagued by atmospheric artifacts (Zebker et al, 1997; Hanssen, 2001). Usually atmospheric artifacts are related with particular epochs and not spatially correlated through time (Zhong lu et al., 2005). Phase delay by atmospheric artifacts could be estimated and removed from the interferograms using meteorological data or continuous GPS data (Williams et al., 1998). Unfortunately, we did not get meteorological data or GPS data for this study area, so adopted least square inversion solution (Menke, 1989) to reduce the effects of atmospheric artefacts as given by

$$Gm = d \quad (1)$$

$$m = \left[G^T G\right]^{-1} G^T d = \begin{bmatrix} N & \sum Z_i \\ \sum Z_i & \sum Z_i^2 \end{bmatrix}^{-1} \begin{bmatrix} \sum d_i \\ \sum Z_i d_i \end{bmatrix} \quad (2)$$

where $G = [Z_1, Z_2, ..., Z_n]$ is a system matrix, each row correspond to an interferogram, while rows represent from start date to end date of each interferogram. In the case of $G_k = G_{d_i} - G_{d_j}$ interferogram, the values of columns i and j are +1 and -1, respectively, and other values are all zero. $d = [d_1, d_2, ..., d_n]$ is known incremental range change value for differential interferogram and $m = [m_1, m_2]$ is unknown deformation value.

For the retrieval of a temporal deformation sequence, we used singular value decomposition.

$$Gv = \phi / \Delta t \quad (3)$$

$$v = \left[G^T G\right]^{-1} G^T \phi / \Delta t \quad (4)$$

As with (1), G is a system matrix, Δt is time interval between interferograms, ϕ is the phase difference with corresponding time interval, and v is the mean velocity estimated by singular value decomposition.

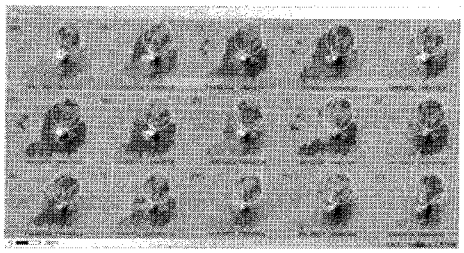

Figure 2. Differential interferograms using ERS-1 and 2 data from 1992 to 2005.

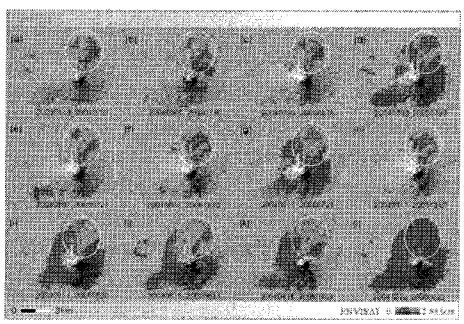

Figure 3. Twelve ENVISAT differential interferograms from 2003 to 2005.

2.4 DInSAR deformation by time series

Augustine volcano has been detected terrain displacements at north portion of island by pyroclastic flow deposits since 1986's eruption. We invert 63 differential interferograms derived from ERS-1, ERS-2 (track 229) and ENVISAT (track 2229) satellite data for a time-dependent deformation signal in the Augustine Island from June 1992 to August 2005. The time-dependent deformation is calculated by performing a linear inversion that solves for the incremental range change between SAR scene acquisitions. We selected coherent points from all interferograms (track 229 and track 2229) for applying least square inversion for reduce atmospheric artifacts and singular value decomposition for the retrieval of a temporal deformation sequence (Figure 4). Figure 4 shows 40 selected coherent points, point-15 represents reference point which means stable area of Augustine Island.

Image of center of Figure 4 was created by averaging all the unwrapped interferograms (track 164, 207, 229, 436 and 501 of ERS-1 and ERS-2 data) spanning one year during the period from June 1992 to November 2005. The graphs on the left of Figure 4 show the deformation history for points 6, 14 and 19 after applying least square inversion and singular value decomposition methods. These three points exhibit the most deformation with around 20.7cm, 36.5cm and 18.8cm (LOS direction) for approximately 13 years, respectively. Black lines represent real values of temporal deformation while blue lines represent values produced by deformation history by second order polynomial equation. This deformation maybe caused by compaction or contraction of 1986's pyroclastic flow deposits that was occur to terrain subsidence at north part of Augustine Island. The reason of total subsidence's difference according to each point dues to the thickness distribution of pyroclastic flow deposits (Masterlark et al., 2006). Bottom side graphs of Figure 4 display the deformation history for point 10, 12 and 13 located on the south and west portions of Augustine Island. These points represent the least amount of deformation with -0.6cm, 1.9cm and 1.6cm (LOS direction) during the period from 1992 to 2005. Because, there has no pyroclastic flow deposits and these points near to reference point (point 15) than other points, relatively. The graphs on the right of Figure 4 show the deformation history for points 11, 16 and 17 which is located to the east side of the Augustine Volcano. These points show a slight amount of inflation with about 5.9cm, 6.2cm and 5.3cm (LOS direction) of deformation from 2001, respectively.

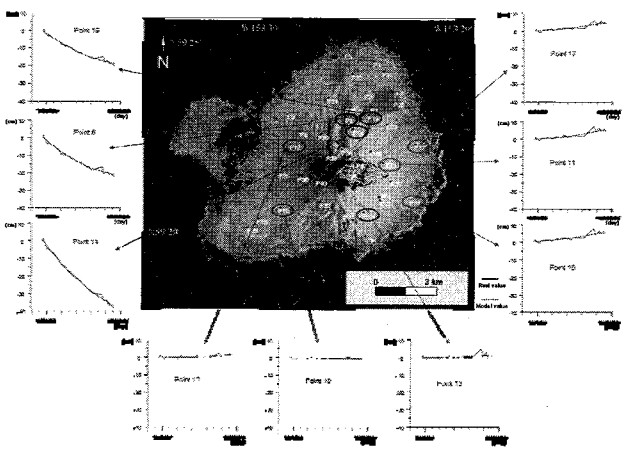

Figure 4. This image is averaging all the unwrapped interferograms. The graphs out of the image show the deformation history.

2.5 InSAR results (After 2006 eruption)

Figure 5 shows subsidence at the northern portion by Pyroclastic flow deposits after 2006 eruption. Even though the interferogram has around 4 month's period from April 29, 2006 to August 12, 2006, purple circle's area in the interferogram represents about 2 fringes.

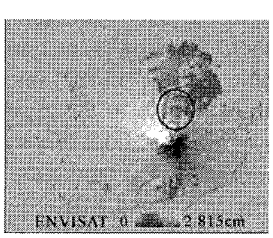

Figure. 5 This interferogram made by April 29, 2006 and August 12, 2006 ENVISAT SAR images.

3. DISCUSSION

Terrain displacement at the Augustine Volcano, Alaska has been measured by InSAR technique from 1992 to

2005 since eruption of 1986. Volcano has three mechanisms for eruption that is pre-eruption, co-eruption and post-eruption stage and we can make inteferograms by each stage. Generally, most of volcanoes have inflation due to volcano surface uplift by accumulation of magma within a shallow reservoir at the pre-eruption stage (Lu et al., 2005) and it represents decreasing pulse signal at range direction in the interferograms. Co-eruption stage has surface displacements due to pyroclastic flow deposits, block & ash flows, and lava flow deposit and this deformation displays several fringes or decorrelation by low coherence in the interferograms. Interferograms of post-eruption stage have increasing range values around summit of volcano due to withdrawal of magma depressurized the reservoir (Lu et al., 2005) and portion of pyroclastic flow deposit of volcano owing to compaction and thermoelastic contraction of pyroclastic flow by a pyroclastic flow gravity load and cooling following emplacement (Lu et al., 2005; Masterlark et al., 2006). In other words, these increasing range values represent subsidence of pyroclastic flow deposit's portion in the interferograms. The difference of between compaction and thermoelastic contraction is on the order of time (Masterlark et al., 2006). Compaction of pyroclastic flow deposits correspond to the order of hour to days about porosity reduction (Rowley et al., 1981), while thermoelastic contraction corresponds to the order of years (Turcotte et al., 1982).

Using InSAR technique, in result of measured subsidence from 1992 to 2005 at the pyroclastic flow deposits' area, subsidence mode was shown definitely as with other volcanoes owing to transient poroelastic deformation, transient viscoelastic deformation and thermoelastic deformation (Masterlark et al., 2006). In case of transient poroelastic deformation effect to pyroclastic flow deposits for a short period of time due to shallow and local flow system by gravity load (Lu et al., 2004). The other deformation mechanisms, viscoelastic and thermoelastic deformation have constant deformation for pyroclastic flow deposits and have an effect on subsidence distribution according to thickness of pyroclastic flow deposits (Masterlark et al., 2006).

4. CONCLUSION

We measured surface deformation of Augustine Volcanic Island, Alaska, using ERS and ENVISAT data the period from June 1992 to December 2005. We used least square (LS) and singular value decomposition (SVD) method for reduces atmospheric artifacts and the retrieval of a temporal deformation sequence. The 1986 pyroclastic flow deposits of Augustine Volcano had experienced the most significant deformation. Subsidence rates were about 0.9-2.8 cm per a year and subsidence distribution according to region due to difference of pyroclastic flow deposits' thickness. The reason of subsidence prefers viscoelastic and thermoelastic deformation by constant deformation to poroelastic deformation by gravity load during short term. The Augustine Volcano showed inflation at eastern part of Island during June 2001 through December 2005 before the 2006 eruption. After 2006 eruption, northern part of Augustine Volcano had subsidence for Pyroclastic flow deposits again.

5. ACKNOWLEDGEMENTS

This study was supported by the Korea Research Foundation Grant funded by the Korea Government (MOEHRD) (KRF-2005-213-C00044) and U. S. Geological Survey (USGS) centre for Earth Resources Observation and Research (EROS). ERS-1 and ERS-2, ENVISAT images are copyright European Space Agency (ESA) and Alaska SAR Facility (ASF).

REFERENCES

Begét, J.E., Kowalik, Z., 2006. Confirmation and Calibration of Computer Modeling of Tsunamis Produced by Augustine Volcano, Alaska. Science of Tsunami Hazards, vol. 24, NO. 4, pp. 257.

Casadevall, T.J., ed., 1994. Volcanic ash and aviation safety-Proceedings of the First International Symposium on Volcanic Ash and Aviation Safety: U.S. Geological Survey Bulletin 2047. pp 450.

Christopher, F.W., Richard B.W., 1998. Preliminary Volcano-Hazard Assessment for Augustine Volcano, Alaska, pp. 98-106.

Fruneau, B., Achache, J., Delacourt, C., 1996. Observation and modeling of the Saint-Etienne-de-Tinee landslide using SAR interferometry, Tectonophysics, pp. 181-190.

Hanssen, R.F., 2001. Radar Interferometry: Data Interpretation and Error Analysis, pp 308.

Lu, Z., Masterlark, T., Dzurisin, D., 2005. Interferometric synthetic aperture radar study of Okmok volcano, Alaska, 1992-2003: Magma supply dynamics and postemplacement lava flow deformation, vol. 110, NO. B2, B02403.

Massonnet, D., Sinmundsson, F., 2000. Remote sensing of volcanic deformation by radar interferometry from various satellites. Remote sensing of active volcanism, pp. 207-221

Masterlark, T., Lu, Z., Rykhus R., 2006. Thickness distribution of a cooling pyroclastic flow deposit on Augustine Volcano, Alaska: Optimization using InSAR, FEMs, and an adaptive mesh algorithm. Journal of Volcanology and Geothermal Research 150, pp. 186-201.

Menke, W., 1989. Geophysical Data Analysis: Discrete Inverse Theory, pp 289.

Miller, T.P., McGimsey, R.G., Richter, D.H., Riehle, J.R., Nye, C.J., Yount, M.E., Dumoulin, J.A., 1998. Catalog of the historically active volcanoes of Alaska. US Geological Survey Open-File Report 98-0582.

Power, J.A., Nye, C.J., Coombs, M.L., Wessels, R.L., Cervelli, P.F., Dehn, J., Wallace, K.L., Freymueller, J.T., and Doukas, M.P., 2006. The reawakening of Alaska's Augustine Volcano: Eos, vol. 87, no. 37, pp. 373-377.

Rowley, P.D., Kuntz, M.A., Macleod, N.S., 1981. Pyroclastic-flow deposits. In: Lipman, P.W., Mullineaux, D.R. (Eds.), The 1980 Eruptions of Mount St. Helens, Washington, U.S. Geological Survey Professional Paper, vol. 1250, pp.489-512.

Tarayre, H., Massonnet, D., 1996. Atmospheric propagation heterogeneities revealed by ERS-1 interferometry. Geophysical Research Letters, vol. 9, pp. 989-992.